ISTFA™ 2017: Proceedings from the
43rd International Symposium for Testing and Failure Analysis
November 5–9, 2017, Pasadena, California, USA

www.asminternational.org

Automated end-point detection and targeted Ar^+ milling of advanced integrated circuit FIB TEM specimens

C.S. Bonifacio, P. Nowakowski, M.J. Campin, J.T. Harbaugh, M. Boccabella, and P.E. Fischione
E.A. Fischione Instruments, Inc., Export, PA 15632 USA

Abstract

The sub-nanometer resolution that transmission electron microscopy (TEM) provides is critical to the development and fabrication of advanced integrated circuits. TEM specimens are usually prepared using the focused ion beam, which can cause gallium-induced artifacts and amorphization. This work presents the use of a concentrated argon ion beam for reproducible TEM specimen preparation using automatic milling termination and targeted ion milling of device features; the result is high-quality and electron-transparent specimens of less than 30 nm. Such work is relevant for semiconductor product development and failure analysis.

Introduction

Advanced integrated circuits (ICs) commonly include fin field effect transistors (FinFET) that are composed of multigate transistors with the source/drain (S/D) channels surrounded by a three-dimensional gate. State-of-the-art ICs are at the 10 nm node; the 7 nm node is at the development stage [1]. At the 10 nm node, the source-drain channel or "fins" are 25% taller and 25% more closely spaced than the 14 nm node [2]. Such high-aspect ratio and complexity of the FinFET structure make metrology and physical failure analysis challenging. Accurately measuring the structure of advanced ICs requires transmission electron microscopy (TEM) due to the resolution it provides. Failure analysis methods and process integration involve TEM characterization for critical dimension (CD) measurements and imaging. Therefore, TEM is critical for the development of advanced ICs. TEM specimen thickness of less than 20 nm is required to characterize the 3D structures of the gate oxide of a FinFET [3].

TEM specimens are usually prepared using a focused ion beam (FIB) due to the site specificity and the accuracy of specimen thinning and extraction that it provides [4, 5]. However, Ga^+ ion milling causes artifacts such as surface amorphization and ion-implanted layers that subsequently limit analytical and high-resolution electron microscopy. In this work, we present Ar^+ ion milling to polish electron-transparent TEM specimens, previously prepared by FIB, using a step-wise process of automated end-point detection and targeted ion milling of the fin structure from a 14 nm node FinFET.

Discussion

Specimen preparation
An Intel Broadwell core M processor was depackaged and from it a cross-section specimen was created using the inverted method [6] in the FIB. Specimen thickness ranging from 200 nm to 150 nm was achieved after 5 kV polishing in the FIB. The specimen was then thinned with a 600 nm diameter argon beam in an ion milling system, the Model 1080 PicoMill® TEM specimen preparation system [E.A. Fischione Instruments, Inc.], with an automatic end-point detection feature. The specimen was mounted on a TEM specimen holder that is compatible with both the ion mill and the TEM goniometer. The ion milling system includes a LaB_6 electron source and various electron detectors (secondary electron detector [SED], scanning transmission electron microscope [STEM], and backscatter electron detector [BSED]), which allow for in situ imaging while ion milling. The small beam of argon ions is directed towards the leading edge of the specimen – in this instance, the Si substrate.

Automatic milling end point
The ion milling system's automatic termination functionality is based on the change in 8-bit gray scale intensity identified by the SED or STEM detector. First, the user inputs a threshold value that is a percentage of the amount of material to be removed. Once milling begins, the system captures a Baseline intensity on the feature of interest on the image. When the intensity value from the live image exceeds or falls below the Baseline intensity value by more than the initial threshold value for a configurable consecutive number of frames, the milling process is terminated.

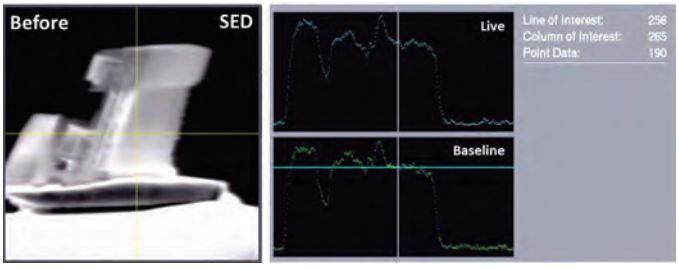

Figure 1: Screenshot from the ion milling system showing in situ SED imaging during 980 eV milling. The difference between the Baseline and Live gray scale intensity values at the point data are compared to the initial threshold value and used to determine the end point of the milling process.

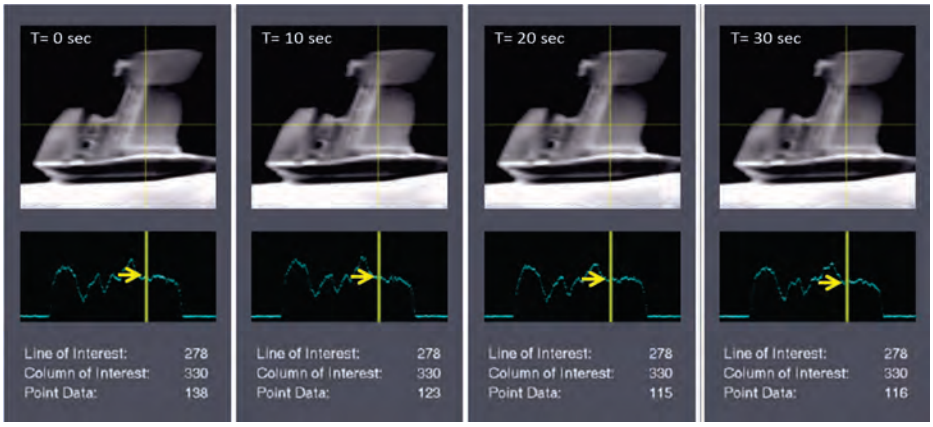

Figure 2: In situ SED imaging during 700 eV milling using the ion milling system. In this series of screen captures, the point data value (marked as arrows on the gray scale plot) decreases as milling time increases, which indicates a change in the gray scale intensity.

In this experiment, the first step was to establish the dynamic range of the image by adjusting the milling system's brightness and contrast settings so that the minimum and maximum gray scale intensity values of the Baseline (see Figure 1) were not cut off. Once the image settings were adjusted, the Baseline was captured, the Line of Interest and the Column of Interest guides were then positioned so that they intersected at the feature of interest (the specimen's silicon substrate was initially selected). The intensity of the live image at the feature of interest was measured and displayed as Point Data (see Figure 1). The value of the point data was 190 on a scale of 0 to 255, with 0 = vacuum and 255 = the thickest material displayed in the image, which in this instance was the specimen grid. The milling system then compared the difference in the gray scale intensity between the Baseline and the Live real-time gray scale intensity (see Figure 1) at the feature of interest to the initial threshold value and determined the milling end point.

Small, incremental threshold values at decreasing energies were used for milling from 980 eV, 900 eV to 700 eV with automatic end-point detection. In Figure 2, the change in live intensity (138 at time = 0 sec to 116 at time = 30 sec) was detected by the ion milling system and resulted in automatic termination of milling. Furthermore, the feature of interest's point data value decreased as the specimen was milled as shown in Figure 2. The feature of interest's decreasing point data values as the specimen was milled is an indication of specimen thinning at the milling location.

Targeted ion milling

Subsequent targeted milling at 500 eV and 300 eV was performed. During these low-energy milling steps, the FinFET structure was used as the feature of interest, that is, the new position for the live point data. In situ imaging with the STEM detector during ion milling (Figure 3) allowed for targeting of the FinFET structure. The increase in contrast on the Si substrate, which was similar to the signal from vacuum, was an indication of the reduction in specimen thickness. The high magnification STEM detector image following 300 eV milling (Figure 3) shows the initially dark metal lines (metal line 2 [M2] and metal line 4, [M4]) became lighter in contrast.

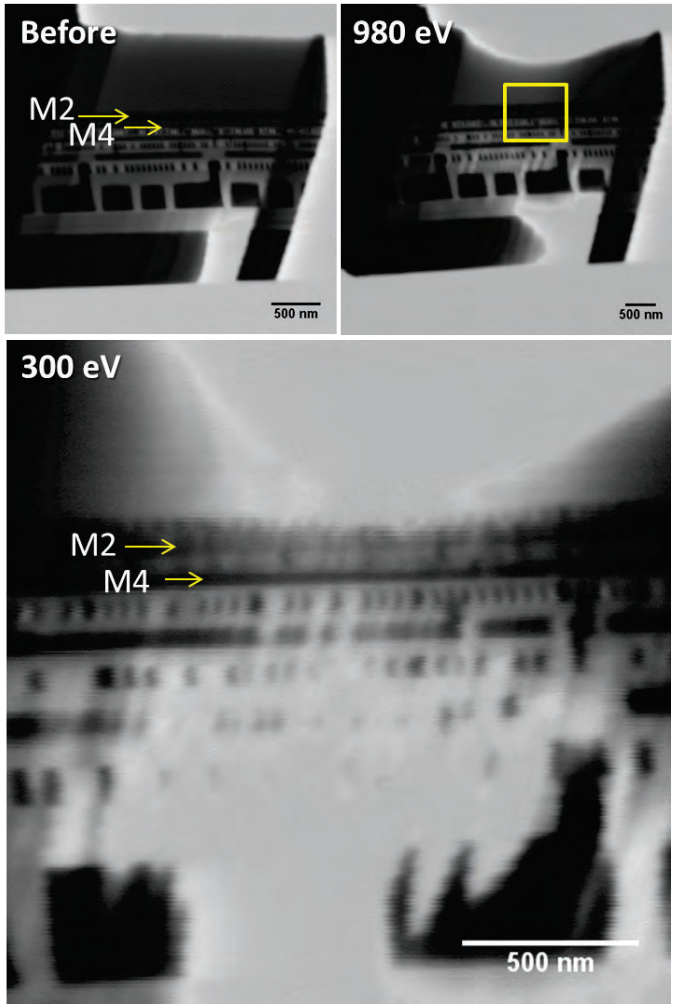

*Figure 3: STEM images in the ion milling system acquired before and after 980 eV and 300 eV milling. The thinnest area after 300 eV milling operations is marked in the 980 eV image. The Si substrate is at the top of the image. Note the difference in contrast of metal line 2 (M2) and Metal line 4 (M4) in the **Before** and the **300 eV** images. The lighter contrast is an indication of a reduction in specimen thickness.*

TEM characterization

TEM images acquired between milling steps at decreasing energies displayed the transition from the metal gate structure of the FinFET (after 700 eV milling) into the epitaxial S/D (after 500 eV and 300 eV milling). The disappearance of the TiN layer following the 700 eV milling step and the metal gate structure following the 500 eV milling step (Figure 4) indicates controlled milling, which allows for the targeting of specific IC features. The images shown in Figure 4 were captured using a Tecnai F30 TEM [FEI Company] equipped with an Orius charge-coupled device camera [Gatan, Inc.] operated at 200 kV.

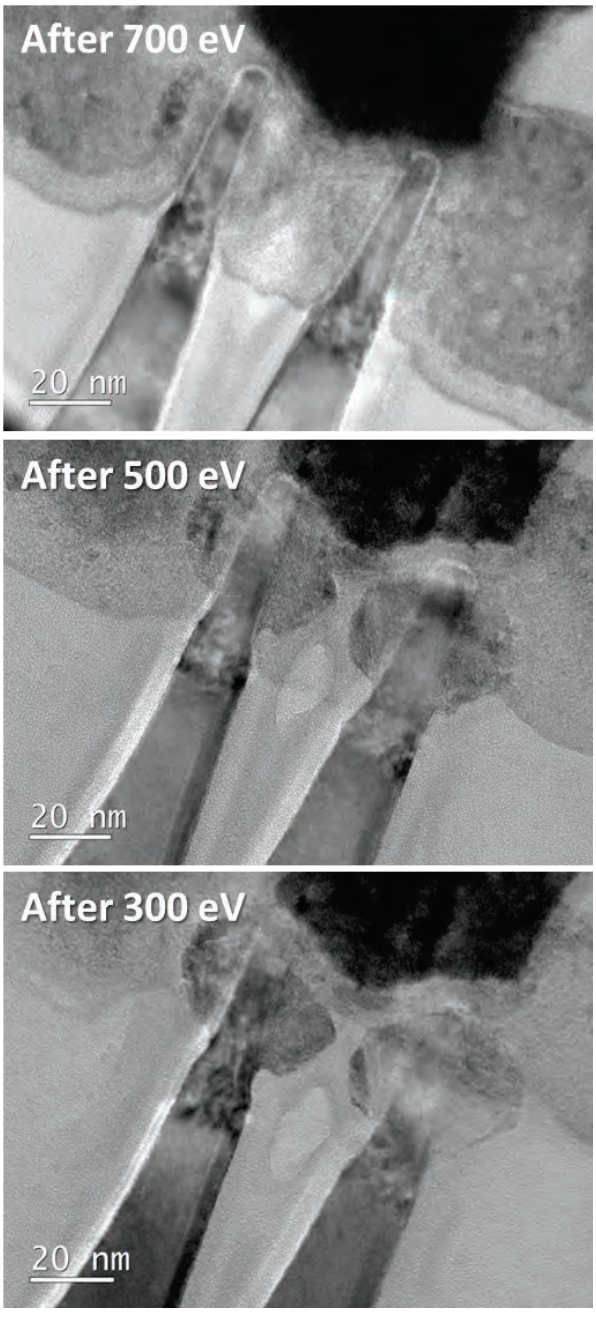

Figure 4: TEM images after 700, 500, and 300 eV milling show the ability to precisely control the progression of milling through the fin structure.

The ion milled specimen was further imaged using an ARM200F aberration-corrected TEM [JEOL, Ltd.] in STEM mode and operated at 200 kV; high-angle annular dark-field (HAADF) and bright-field STEM (BF-STEM) images were acquired simultaneously. HAADF imaging, which is highly sensitive to atomic number (Z), was performed to differentiate the layers of the FinFET structure. Low-magnification images of the FinFET show a homogeneous TEM specimen free from redeposition (Figures 5a and 5b). Figures 5c and 5d are atomic-resolution BF-STEM and dark-field (DF-STEM) images, respectively, which show a TEM specimen that is electron transparent. The fast Fourier transform acquired from the Si in the fin (compare to Figure 5e) shows no diffused halo in the background, which usually originates from an amorphous material; therefore, the specimen has an amorphous-free surface. The metal gate over the fin and TiAl grains is pronounced and distinct in Figures 5a and 5b. Figures 5c and 5d show the atom columns of Si in the fin and amorphous high-k (bright layer in BF-STEM and dark layer in DF-STEM) and work function setting material (dark layer in BF-STEM and bright layer in DF-STEM) above the fin.

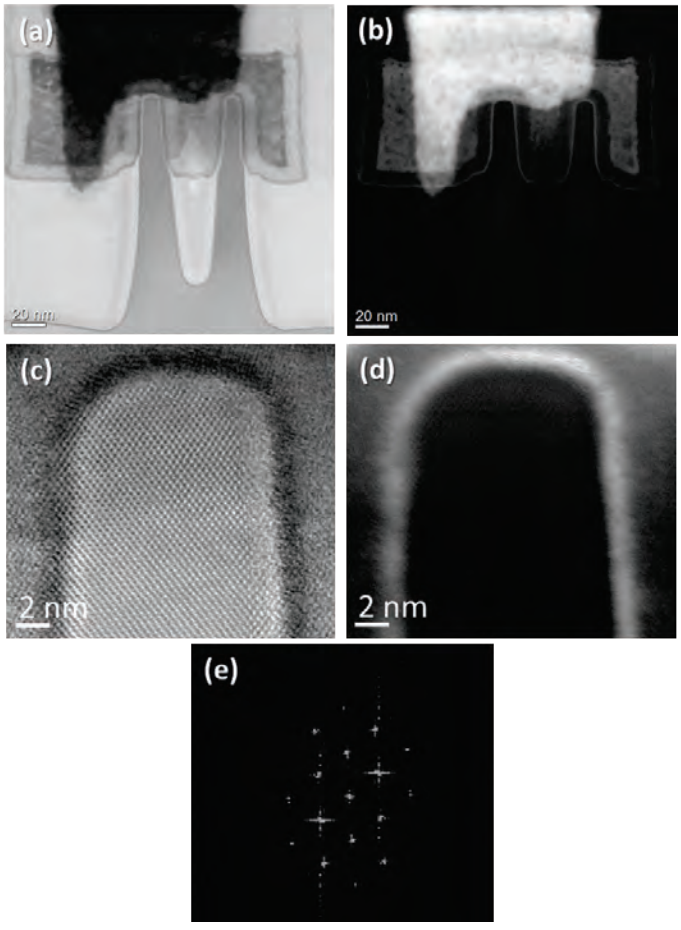

Figure 5: Bright field (a and c) and dark field (b and d) STEM images of the FinFET after ion milling. Fast Fourier transform (e) derived from the Si in the fin.

The thickness of the specimen used for the atomic resolution imaging was determined using electron energy loss spectroscopy. Figures 6a and 6b show an unfiltered energy filtered TEM (EFTEM) image and an associated EFTEM thickness map, respectively. The thickness map is a relative-thickness calculated map based on the ratio of the zero-loss map (not shown) and the unfiltered image (Figure 6a) using the log-ratio method [7]. The relative thickness map is in units of t/λ, where t is the specimen thickness and λ is the inelastic mean free path of the primary beam electrons through each particular material for a given accelerating voltage.

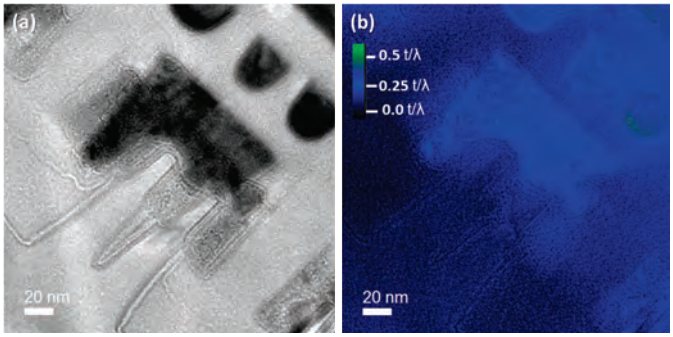

Figure 6: Unfiltered image (a) and energy filtered transmission electron microscope thickness map (b) of the ion milled specimen in Figure 4. The color is based on the t/λ scale.

For comparison, Table 1 shows the thickness values calculated from example relative t/λ values based on a value of λ for Si with 200 keV primary electrons.

Table 1: Calculated specimen thickness, t, given the measured t/λ and inelastic mean free path (MFP) value of 148.121 nm [8] for crystalline Si at 200 kV.

t/λ	Thickness, t [nm]
0.22	32.6
0.17	25.2
0.11	16.3

The overall measured t/λ was less than 0.22 giving the specimen thickness of less than approximately 32.6 nm. The thinnest part of the specimen was at the Si substrate and at the FinFET structure; these locations had t/λ values ranging from 0.22 to 0.11, which correspond to 32.6 to 16.3 nm in thickness (Table 1). The area of the fins is measured as $t/\lambda = 0.17$, which is 25.2 nm. This thickness is equivalent to a point value of 80 using the SED detector on the feature of interest (compare to Figure 2) after 300 eV milling. This thickness value falls within the TEM specimen thickness requirement of at least 20 to 30 nm for TEM imaging of FinFET structures as shown by Feng, et al. [3].

Evaluation of end-pointing methodology

Qualitatively, the reduction of specimen thickness can be related to the change in the overall image intensities during milling. In fact, this is the basis of the automatic end-point detection in the ion milling system. To evaluate this premise, the specimen thicknesses of two Si specimens that were processed using the ion milling system were analyzed.

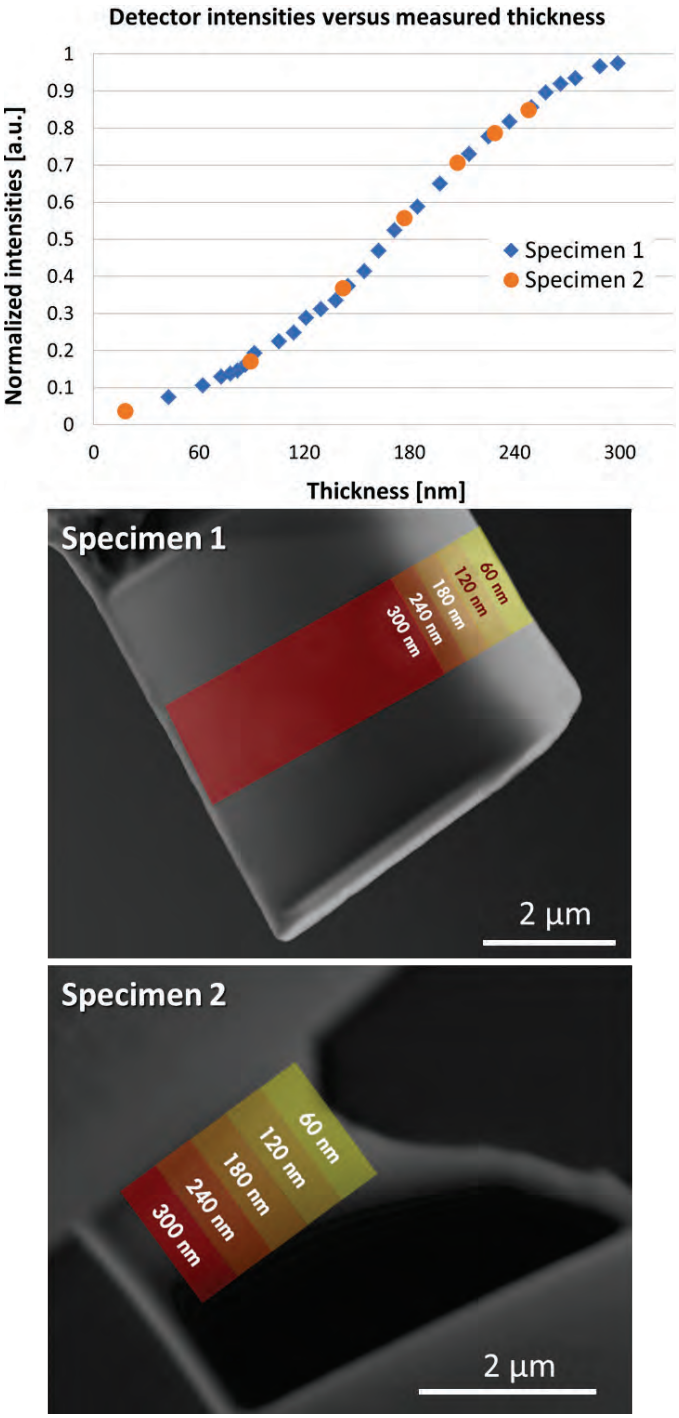

Figure 7: Relationship of the secondary electron detector normalized intensities and the measured specimen thickness using the XPP model. The thickness ranges are overlaid on the SEM images as a representation of the specimens' varying thicknesses after ion milling.

The specimens' thicknesses were determined using the *XPP* model [9, 10], which determines the correlation between layer

thickness and k-ratios measured by energy dispersive X-ray spectroscopy (EDS) technique. This technique has been widely used for thickness determination in the scanning electron microscope (SEM) [11, 12, 13, 14]. The model is implemented in LayerProbe software [Oxford Instruments] used for EDS acquisition. The intensities from the acquired SED images of the two specimens were normalized. These intensities were then plotted and the corresponding thicknesses measured across the Si specimens (Figure 7). The decreasing gray scale intensity values are proportional to the decreasing specimen thickness in the linear region, which validates the methodology behind the automatic end-point detection functionality.

Conclusions

High-quality specimens free from amorphous damage for analytical and high-resolution electron microscopy were obtained using a small Ar^+ ion beam and a step-wise process of automated end-point detection and targeted ion milling was demonstrated. The resulting specimen thickness, less than 30 nm, is suitable for imaging and analysis of FinFET structures.

Acknowledgment

The authors thank Kevin McIlwrath of JEOL USA for STEM image acquisition and Lucille Giannuzzi of EXpressLO LLC for the specimens.

References

[1] Zeitzoff, P. Akarvardar, K., Mody, J., Konar, A., "Metrology Requirements and Challenges for Advanced FinFET Technology: Insight from TCAD Simulations," *Frontiers of Characterization and Metrology for Nanoelectronics,* Monterey, CA, March 2017, pp. 30-32.

[2] Mistry, K.., "10 nm Technology Leadership: Intel Technology and Manufacturing," *Technology and Manufacturing Day*, San Francisco, CA, March 2017.

[3] Feng, H., Low, G.R., Tan, P.K., Zhao, Y.Z., Yap, H.H., Dawood, M.K., Zhou, Y., Du, A.Y., Chen, C.Q., Tan, H., Huang, Y.M., Wang, D.D., Lam, J., Mai, Z.H., "Investigation of Protection Layer Materials for Ex-situ 'Lift-Out' TEM Sample Preparation with FIB for 14 nm FinFET," *Proc 40th Int'l Symp for Testing and Failure Analysis*, Houston, TX, November 2014, pp. 478-482.

[4] Mayer, J., Giannuzzi, L.A., Kamino, T. and Michael, J., "TEM Sample Preparation and FIB-induced Damage," *MRS Bulletin*, Vol. 32, (2007), pp. 400-407.

[5] Giannuzzi, L.A., and Stevie, F.A., "A review of focused ion beam milling techniques for TEM specimen preparation," *Micron*, Vol. 30, (1999), pp. 197-204.

[6] Alvis, R., Blackwood, J., Lee, S-H., Bray, M., "High-throughput, site-specific sample prep of ultra-thin TEM lamella for process metrology and failure analysis," *Proc 38th Int'l Symp for Testing and Failure Analysis*, Phoenix, AZ, November 2012, pp. 391-398

[7] Egerton, R. F., *Electron energy-loss spectroscopy in the electron microscope 3rd edition*, Springer (New York, 2011).

[8] Iakoubovskii, K., Mitsuishi, K., Nakayama, Y. and Furuya, K., "Thickness measurements with electron energy loss spectroscopy," *Microsc Res and Tech*, Vol. 71, (2008), pp. 626–631.

[9] Pouchou, J.L., Pichoir F.," X-ray microanalysis of stratified specimens," *Anal Chim Acta*, Vol. 283, (1993), pp. 81–97.

[10] Pouchou, J.L., Pichoir F., "Electron probe X-ray microanalysis applied to thin surface films and stratified specimens," *Scanning Microsc Suppl* , Vol. 7, (1993), pp. 167–89.

[11] Nowakowski, P., Bonifacio, C.S., Campin, M.J., Ray, M.L., and Fischione, P.E., "Accurate removal of implanted gallium and amorphous damage from TEM specimens after focused ion beam (FIB) preparation," *Microsc Microanal,* Vol. 23 (Suppl 1), (2017), pp. 300-301.

[12] Nowakowski, P., Christien, F., Allart, M. Borjon-Piron, Y., Le Gall, R. "Measuring grain boundary segregation using wavelength dispersive X-ray spectroscopy: Further developments," *Surface Science,* Vol. 605, (2011), pp. 848-585.

[13] Hiscock, M., Dawson, M., Lang, C., Hartfield, C., Statham, P., "In-Situ Quantification of TEM Lamella Thickness and Ga Implantation in the FIB," *Microsc Microanal*, Vol. 20 (Suppl 3), 2014, pp.342-343.

[14] Christien, F., Ferchaud, E., Nowakowski, P., Allart, M. Use of Electron Probe MicroAnalysis to Determine the Thickness of Thin Films in Materials Science, X-Ray Spectroscopy, Dr. Shatendra K Sharma (Ed.), *InTech* (2012), pp.101-118.